

Mirror Symmetry in Integral Formulations for Eddy Currents

Mauro Passarotto¹, Daniel Klis², Oliver Rain², and Ruben Specogna¹

¹Polytechnic Department of Engineering and Architecture (DPIA), EMCLab, Università di Udine, 33100 Udine, Italy

²Robert Bosch GmbH, 71272 Renningen, Germany

This contribution addresses the exploitation of mirror symmetry (formally, the abelian D_1 and D_2 dihedral symmetry groups) in various integral formulations for eddy current problems. The novelty of the contribution is in particular how to rigorously treat non-simply-connected conductors when computing the first cohomology group generators on the symmetry cell of the problem only.

Index Terms—Cohomology, eddy currents, finite element method–boundary element method (FEM–BEM), integral formulations, mirror symmetry.

I. INTRODUCTION

EXPLOITING symmetry has been recognized as an effective method to save a sensible amount of simulation time. It allows to solve the problem on a given domain \mathcal{K} by solving a family of problems on a *symmetry cell* \mathcal{S} instead. It is impossible to survey all the literature, so we just mention [1] for the finite element method (FEM) and [2] for a FEM–boundary element method (FEM–BEM) based on the magnetic vector potential.

This article considers the efficient boundary integral (BI) formulation for solving eddy current problems, which employ a magnetic scalar potential [3], the volume integral (VI) formulation based on the electric vector potential [4], and the FEM–BEM in [5]. These three methods are quite different, but they share the necessity of computing the so-called *cohomology generators* [5]–[7] to obtain a consistent design of electromagnetic potentials.

The purpose of this article is to present the details of cohomology computation in relation to the exploitation of mirror symmetry, i.e., the abelian D_1 and D_2 dihedral symmetry groups, in the aforementioned integral formulations for eddy currents. For example, Fig. 1 represents a conductor with D_2 symmetry. Similar to the standard solution surveyed in [2], the starting point is to have a matrix which is *block-circulant*. The main issue is that in the three considered formulations this is not true in general because of the presence of nonlocal constraints due to cohomology.

The general idea to get a block-circulant matrix even in presence of non-simply-connected domains, introduced in [6] and [7] for cyclic symmetry, is that the representatives of the cohomology generators must share the same symmetry of the problem. Yet, the case of mirror symmetry is quite different with respect to cyclic symmetry because the solution introduced in [6] and [7], based on the identifications of the elements in the two symmetry parts of the boundary

of \mathcal{S} , cannot be used here as it may be deduced by looking at \mathcal{S} of Fig. 1. Hence, since the idea of the *topological stitching* applied to cyclic symmetry cannot be considered, the algorithm for the computation of cohomology generators required for this application must be inspired to something different than what proposed in [6] and [7].

We observe that the techniques for cohomology computation presented so far in literature, derived from the Hiptmair–Ostrowski (H–O) algorithm [8], compute a basis of *absolute* $H^1(\partial\mathcal{K})$ generators—with $\partial\mathcal{K}$ being a triangulated surface **without boundary**—for VI formulations (see [4], [7]) and a basis of the *relative* $H^1(\Sigma, \partial\Sigma)$ cohomology group for surface integral formulations [3], [6], where Σ is the triangulated surface—possibly with boundary—representing the thin conductor. Differently, the efficient computation of absolute $H^1(\Sigma)$ generator, **when Σ has a boundary**, is required in the present case for exploiting mirror symmetry with the integral formulations here considered and, as far as we know, this aspect has not been treated yet: this contribution aims at filling that gap.

In Section II, we first introduce a proper set of equations to study eddy currents by using either the VI or the FEM–BEM approach. Then, the very idea to compute the required representative of absolute $H^1(\Sigma)$ generators is exposed in Section III. Then, the proposed approach and described implementation are validated by exposing the numerical results in Section IV: the agreement of the solutions obtained by considering either the full conductive structure \mathcal{K} or the symmetry cell \mathcal{S} only is verified by solving eddy currents on the conducting plate with holes of Fig. 1 with both the VI formulation and FEM–BEM. In addition, we carry out the same comparison (solution on \mathcal{K} versus \mathcal{S}) when using the FEM–BEM approach to study the behavior of an electromagnetic valve.

II. VI AND FEM–BEM FORMULATIONS

A. VI Formulation

We now briefly present the VI formulation to study eddy currents in the frequency domain, which some of the numerical results are referred to. We consider the equations detailed in [9]

Manuscript received November 30, 2020; revised January 20, 2021; accepted March 5, 2021. Date of publication March 10, 2021; date of current version May 17, 2021. Corresponding author: M. Passarotto (e-mail: passarotto.mauro@spes.uniud.it).

Color versions of one or more figures in this article are available at <https://doi.org/10.1109/TMAG.2021.3065253>.

Digital Object Identifier 10.1109/TMAG.2021.3065253

0018-9464 © 2021 IEEE. Personal use is permitted, but republication/redistribution requires IEEE permission.

See <https://www.ieee.org/publications/rights/index.html> for more information.

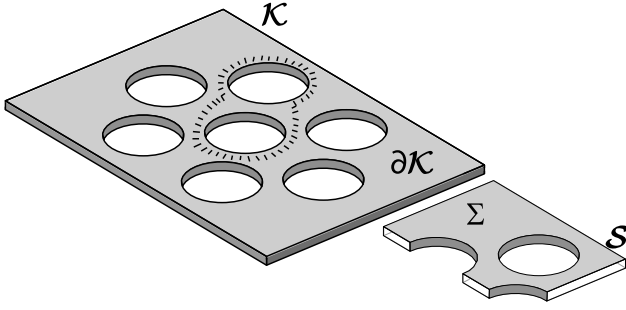


Fig. 1. Top: an example of symmetric nontrivial conducting domain \mathcal{K} and its boundary $\partial\mathcal{K}$, i.e., a surface without boundary. Right corner: the symmetry cell \mathcal{S} and its boundary $\Sigma = \partial\mathcal{K} \cap \partial\mathcal{S}$, a surface with boundary.

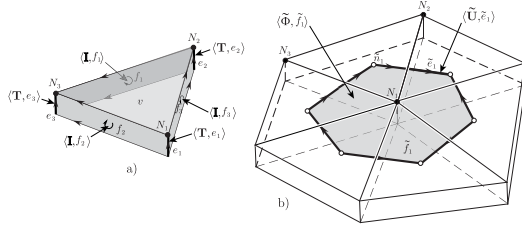


Fig. 2. (a) Primal geometrical elements of a primal volume of the mesh. (b) Dual geometrical elements construction and identification.

that derive from the use of the compatible numerical method more extensively exposed in [10].

Given a non-simply-connected domain Ω_c , the considered framework requires to encode it into a cell complex \mathcal{K} , which will be hereafter considered as the *primal* grid, that distinguishes from its barycentric *dual* subdivision denoted as $\tilde{\mathcal{K}}$. These cell complexes will be, respectively, formed by N_v primal volumes v , N_f primal faces f , N_e edges e and N_n nodes n and by N_n dual volumes \tilde{v} , N_e dual faces \tilde{f} , N_f dual edges \tilde{e} and N_v dual nodes \tilde{n} (see Fig. 2).

The vector of the currents flowing through the faces of \mathcal{K} is

$$\mathbf{I} = \mathbf{C}(\mathbf{T} + \mathbf{H}\mathbf{i}) \quad (1)$$

where \mathbf{T} denotes the array of the degrees of freedom (DOF) storing the integral of the electric vector potential along the edges of \mathcal{K} , \mathbf{C} is a face-edge incidence matrix that also configures as a discrete curl operator, \mathbf{i} the array of the independent currents flowing in Ω_c and where the matrix \mathbf{H} stores all the representatives of the generators that constitute a basis of the first cohomology group $H^1(\partial\mathcal{K})$.

Then, by introducing the two discrete constitutive relations $\tilde{\mathbf{U}} = \mathbf{R}\mathbf{I}$ and $\tilde{\mathbf{A}} = \mathbf{M}\mathbf{I}$ linking \mathbf{I} to the array of the electromotive force $\tilde{\mathbf{U}}$ along the edges of $\tilde{\mathcal{K}}$ and to the array of the integral of the magnetic vector potential $\tilde{\mathbf{A}}$ still along the edges of $\tilde{\mathcal{K}}$ and by enforcing Faraday's law in its local and nonlocal forms

$$\mathbf{C}^T \tilde{\mathbf{U}} + i\omega \tilde{\Phi} = \mathbf{0} \quad (2)$$

$$\mathbf{H}^T (\mathbf{C}^T \tilde{\mathbf{U}} + i\omega \tilde{\Phi}) = \mathbf{0} \quad (3)$$

where $\tilde{\Phi}$ is the magnetic flux through the faces of $\tilde{\mathcal{K}}$, the final system of equations to be solved is

$$\begin{bmatrix} \mathbf{K} & \mathbf{KH} \\ \mathbf{H}^T \mathbf{K} & \mathbf{H}^T \mathbf{KH} \end{bmatrix} \begin{bmatrix} \mathbf{T} \\ \mathbf{i} \end{bmatrix} = \begin{bmatrix} \mathbf{b}_s \\ \mathbf{H}^T \mathbf{b}_s \end{bmatrix}. \quad (4)$$

In this last expression $\mathbf{K} = \mathbf{C}^T (\mathbf{R} + i\omega \mathbf{M}) \mathbf{C}$ and $\mathbf{b}_s = -i\omega \mathbf{C}^T \tilde{\mathbf{A}}_s$ wherein $\tilde{\mathbf{A}}_s$ is the integral of the magnetic vector potential along $\tilde{\mathcal{K}}$ edges produced by a known magnetic source such as a coil crossed by a known current or such as a variable imposed magnetic field. In addition, to achieve (4) it is necessary to rewrite the flux of the magnetic induction field across the dual faces \tilde{f} as $\tilde{\Phi} = \mathbf{C}^T \tilde{\mathbf{A}}$.

Consequently, in this article, we focus on the computation of the matrix \mathbf{H} of (4) when Ω_c shows a mirror symmetry and so the matrix storing the representatives of the cohomology generators can be computed by referring to the symmetry cell \mathcal{S} only. This is achieved by retrieving the generators of $H^1(\Sigma)$.

B. FEM-BEM

The symmetric FEM-BEM eddy current formulation written in terms of magnetic vector potential, following [5], leads to a system of equations of the form:

$$\begin{bmatrix} \mathbf{S} + i\omega \mathbf{P} + \mathbf{N} & \mathbf{L} - \frac{1}{2} \mathbf{B} \\ \mathbf{L}^T - \frac{1}{2} \mathbf{B}^T & \mathbf{V} \end{bmatrix} \begin{bmatrix} \mathbf{A}_{\text{FEM}} \\ \Psi_{\text{BEM}} \end{bmatrix} = \begin{bmatrix} \mathbf{i}_s \\ \mathbf{0} \end{bmatrix} \quad (5)$$

where \mathbf{S} and \mathbf{P} are the standard sparse FEM stiffness and mass matrices, \mathbf{B} is a sparse coupling matrix, and \mathbf{N} , \mathbf{L} as well as \mathbf{V} are dense BEM operators. \mathbf{A}_{FEM} and Ψ_{BEM} stems from the arrays of the DOF representing, respectively, the unknown magnetic vector potentials and the unknown values of the nodal stream functions. The right-hand side models an imposed current source \mathbf{i}_s .

Yet, equations in (5) are valid *iff* the computational domain is simply connected. This stems from the fact that electrical surface current density associated with Ψ_{BEM} is discretized using, on the mesh surface $\Gamma = \partial\mathcal{K}$, divergence-free trial functions $H(\text{div}_0, \Gamma)$. Differently, for a non-simply-connected domain, nonlocal relations also have to be considered in a similar way to that one previously developed and described for the VI formulation. Hence, in general, expressing this nonlocal basis requires also, in this case, the calculation of a representative of absolute $H^1(\Gamma)$ cohomology generators, where Γ is a surface without boundary. The generators, encoded into \mathbf{H} leads to additional blocks of the system $\mathbf{H}^T \mathbf{V} \mathbf{H}$ and $\eta_{\mathbf{H}}$, $\theta_{\mathbf{H}}$ that, as in (4), are a linear combination of \mathbf{H} with the left-hand side of (5).

In conclusion, the system to be solved becomes

$$\begin{bmatrix} \mathbf{S} + i\omega \mathbf{P} + \mathbf{N} & \mathbf{L} - \frac{1}{2} \mathbf{B} & \eta_{\mathbf{H}} \\ \mathbf{L}^T - \frac{1}{2} \mathbf{B}^T & \mathbf{V} & \theta_{\mathbf{H}} \\ \eta_{\mathbf{H}}^T & \theta_{\mathbf{H}}^T & \mathbf{H}^T \mathbf{V} \mathbf{H} \end{bmatrix} \begin{bmatrix} \mathbf{A}_{\text{FEM}} \\ \Psi_{\text{BEM}} \\ \mathbf{i} \end{bmatrix} = \begin{bmatrix} \mathbf{i}_s \\ \mathbf{0} \\ \mathbf{0} \end{bmatrix} \quad (6)$$

where \mathbf{i} contains the unknown nonlocal surface currents that correspond to the cohomology generators.

Once again, when moving from the complete conducting domain \mathcal{K} to the symmetry cell \mathcal{S} , this last one does not exhibit the same topological properties of \mathcal{K} anymore; the boundary of \mathcal{S} , namely Σ , is a surface that has a boundary, therefore, to try to retrieve the absolute $H^1(\Sigma)$ generator with the usual procedure inspired to the H-O algorithm would not yield an equivalent system with respect to the original one computed on \mathcal{K} instead. To overcome this situation, as for the VI formulation, a new algorithm must be developed to correctly obtain the cohomology generators.

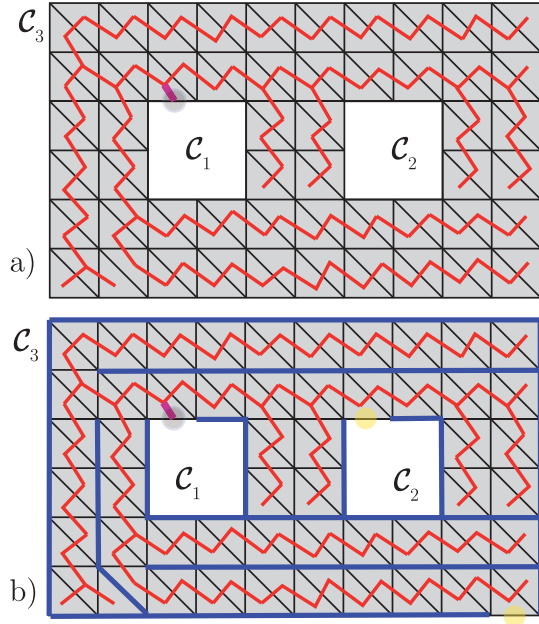


Fig. 3. (a) Tree on the dual edges (in red) is built and joint to one of the connected components C_1 (thick magenta edge). (b) Tree on the free primal edges is built (in blue): two edges on the other connected components C_2 and C_3 not in the primal/dual trees remains (yellow circles).

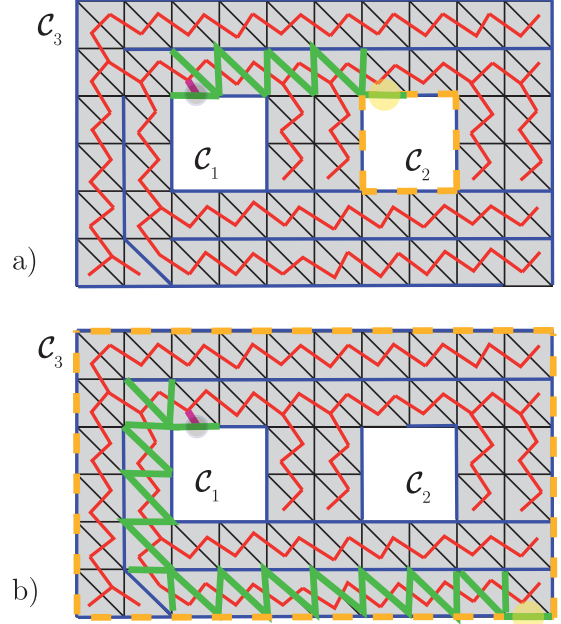


Fig. 4. Starting from a free edge of each connected component sought generators are retrieved starting from (a) C_2 and (b) C_3 .

III. COHOMOLOGY COMPUTATION ON \mathcal{S}

Let us define the duality operator D on Σ as the operator that returns the dual edge \tilde{e} which is dual to a given primal edge e , i.e., $\tilde{e} = D(e)$. The proposed fast and combinatorial algorithm, running in linear time, to find cohomology generators for a surface with boundary is as follows.

- 1) Consider the dual graph which is composed by dual edges which are dual to interior primal edges, i.e., dual edges in the set $\{D(e)|e \in (\Sigma - \partial\Sigma)\}$;
- 2) Find a dual spanning tree \tilde{T} on Σ , i.e., an arbitrary spanning tree on the dual graph [Fig. 3(a), red edges];
- 3) For one edge $b \in \partial\Sigma$ (i.e., a random boundary edge of Σ), put the dual edge $\tilde{b} = D(b)$ in \tilde{T} [Fig. 3(a), thick magenta edge];
- 4) Find a primal spanning tree T on Σ by using as a graph the set of primal edges not in $D^{-1}(\tilde{T})$ [Fig. 3(b), blue edges];
- 5) Find the set \tilde{E} of dual edges not belonging to \tilde{T} and to $D(T)$ [Fig. 3(b), yellow circles];
- 6) Let $\{\tilde{C}(\tilde{e})|\tilde{e} \in \tilde{E}\}$ be a set of dual edges that belong to the dual cycle that originates when considering the graph $\tilde{e} \cup \tilde{T}$. The dual cycle is oriented by assigning a +1 or -1 incidence coefficients to each dual edge of the dual cycle.
- 7) The primal edges $\{D^{-1}(\tilde{C}(\tilde{e}))|\tilde{e} \in \tilde{E}\}$ with the same incidence coefficients are representatives of a basis of the first cohomology group $H^1(\Sigma)$ (Fig. 4, green edges).

IV. NUMERICAL RESULTS

We first present a linear eddy current problem computed in the frequency domain with both VI and FEM-BEM code

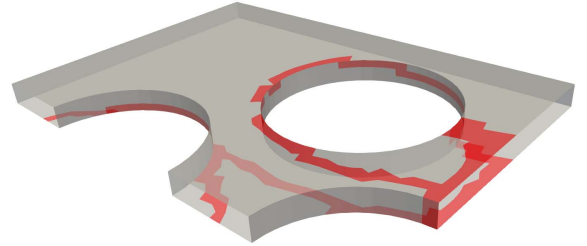


Fig. 5. Support of the representatives of the retrieved generators on \mathcal{S} of Fig. 1. Computation time for the retrieval: less than 1 s.

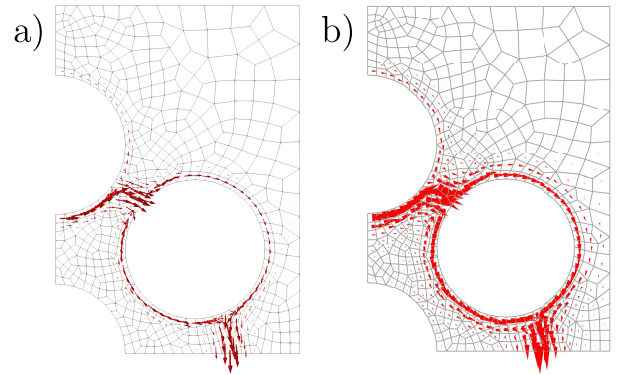


Fig. 6. Real part of the current density flowing in \mathcal{S} of Fig. 1 plate (top view) solved (a) with FEM-BEM and (b) with the VI code.

for the thin plate with holes of Fig. 1 (dimension: $0.7 \times 1.0 \times 0.025$ m). For this simulation, it was used $\rho = 1.68 \cdot 10^{-8} \Omega\text{m}$ as plate resistivity, and a circular wire centered in $(0, 0, 0.035$ m) of radius $r_0 = 0.25$ m as source of magnetic field. The wire is crossed by a sinusoidal current $I_s^{\text{rms}} = 10$ A

TABLE I
OHMIC LOSSES COMPARISON

N_v	VI [mW]		FEM-BEM [mW]	
	Full	Quarter	Full	Quarter
2000	0.785	0.785	0.938	0.932
6000	0.826	0.824	0.926	0.926
11000	0.850	0.850	0.914	0.914

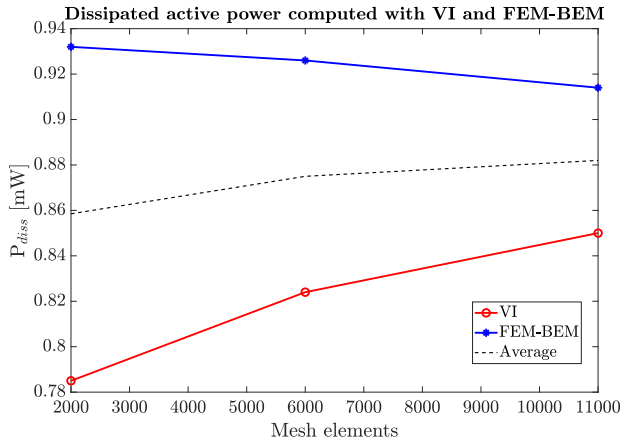


Fig. 7. Dissipated active power P_{diss} computed with VI and FEM-BEM on different meshes of the symmetry cell.

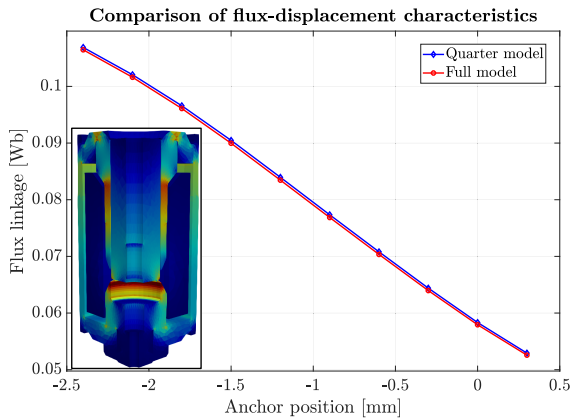


Fig. 8. Flux linkage calculation comparison between full and mirrored model of the valve. Inset: magnetic induction in the valve (quarter model).

at a frequency $f = 50$ Hz. The retrieved generators are shown in Fig. 5 while Fig. 6 shows the current density flowing in S when computed with the two declared approaches. In addition, Table I reports a comparison of the dissipated power in the plate when calculated on the full (\mathcal{K}) or mirrored (\mathcal{S}) cell: an excellent agreement is exhibited. The related power convergence trend is exposed in Fig. 7.

In Figs. 8 and 9 the results of the FEM-BEM simulation of an electromagnetic valve driven by a coil crossed by a $1.2 \cdot 563$ [At] current are reported. The valve housing is

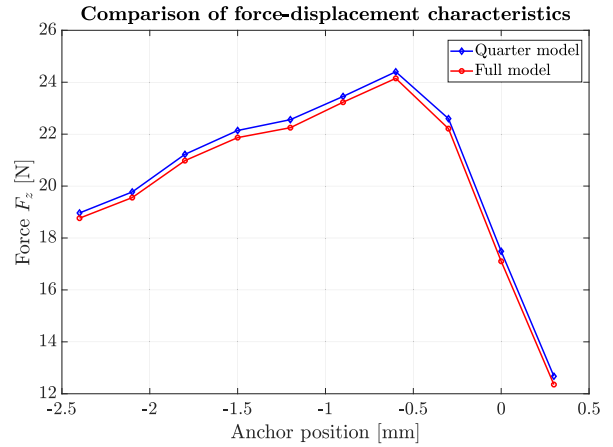


Fig. 9. Electromagnetic force F_z calculation comparison between the full and the mirrored model of the valve.

made of steel, diameter $d = 28.3$ mm, height $h = 36.0$ mm. Both the results obtained considering \mathcal{K} and \mathcal{S} are plotted in terms of flux linkage and in terms of vertical electromagnetic force F_z computed through the Maxwell stress tensor [11]. Apart from the two curves not perfectly superimposed due to the chosen tolerance of Newton's iterative scheme applied to solve the time-domain nonlinear eddy current problem arising from the $B-H$ characteristic of the steel, the comparison substantially confirms the correctness of the proposed approach.

REFERENCES

- [1] A. Bossavit, "Symmetry, groups, and boundary value problems," *Comput. Methods Appl. Mech. Eng.*, vol. 56, no. 2, pp. 167–215, 1986.
- [2] S. Kurz, O. Rain, and S. Rjasanow, "Application of the adaptive cross approximation technique for the coupled BE-FE solution of symmetric electromagnetic problems," *Comput. Mech.*, vol. 32, nos. 4–6, pp. 423–429, Dec. 2003.
- [3] A. Kameari, "Transient eddy current analysis on thin conductors with arbitrary connections and shapes," *J. Comput. Phys.*, vol. 42, no. 1, pp. 124–140, Jul. 1981.
- [4] R. Albanese and G. Rubinacci, "Integral formulation for 3D eddy-current computation using edge elements," *Proc. Inst. Elect. Eng. Phys. Sci., Meas. Instrum., Manage. Educ.*, vol. 135, no. 7, pp. 457–462, Sep. 1988.
- [5] R. Hiptmair, "Symmetric coupling for eddy current problems," *SIAM J. Numer. Anal.*, vol. 40, no. 1, pp. 41–65, Jan. 2002.
- [6] B. Kapidani, M. Passarotto, and R. Specogna, "Exploiting cyclic symmetry in stream function-based boundary integral formulations," *IEEE Trans. Magn.*, vol. 55, no. 6, pp. 1–4, Jun. 2019.
- [7] M. Passarotto and R. Specogna, "Cyclic symmetry in volume integral formulations for eddy currents: Cohomology computation and gauging," *IEEE Trans. Magn.*, vol. 56, no. 2, pp. 1–4, Feb. 2020.
- [8] R. Hiptmair and J. Ostrowski, "Generators of $H_1(\Gamma_h, \mathbb{Z})$ for triangulated surfaces: Construction and classification," *SIAM J. Comput.*, vol. 31, no. 5, pp. 1405–1423, 2002.
- [9] P. Bettini, M. Passarotto, and R. Specogna, "A volume integral formulation for solving eddy current problems on polyhedral meshes," *IEEE Trans. Magn.*, vol. 53, no. 6, pp. 1–4, Jun. 2017.
- [10] L. Codecasa, R. Specogna, and F. Trevisan, "A new set of basis functions for the discrete geometric approach," *J. Comput. Phys.*, vol. 229, no. 19, pp. 7401–7410, Sep. 2010.
- [11] F. Henrotte and K. Hameyer, "Computation of electromagnetic force densities: Maxwell stress tensor vs. virtual work principle," *J. Comput. Appl. Math.*, vol. 168, nos. 1–2, pp. 235–243, Jul. 2004.